

NEOBABEL: AN INCLUSIVE MULTILINGUAL OPEN TOWER FOR VISUAL GENERATION

Anonymous authors

Paper under double-blind review

ABSTRACT

Text-to-image generation advancements have been predominantly English-centric, creating barriers for non-English speakers and perpetuating digital inequities. While existing systems rely on translation pipelines, these introduce semantic drift, computational overhead, and cultural misalignment. We introduce NEOBABEL, a novel multilingual image generation framework that sets a new Pareto frontier in performance, efficiency and inclusivity, supporting six languages: *English, Chinese, Dutch, French, Hindi, and Persian*. The model is trained using a combination of large-scale multilingual pretraining and high-resolution instruction tuning. To evaluate its capabilities, we expand two English-only benchmarks to multilingual equivalents: m-GenEval and m-DPG. NEOBABEL achieves state-of-the-art multilingual performance while retaining strong English capability. Notably, NEOBABEL matches or exceeds English-only models while being 2–4× smaller. We release an open toolkit, including all code, model checkpoints, a curated dataset of 124M multilingual text-image pairs, and standardized multilingual evaluation protocols, to advance inclusive AI research.

1 INTRODUCTION

Recent advances in diffusion models and large-scale vision-language pretraining have revolutionized text-to-image generation, enabling the creation of high-quality images from natural language descriptions (Rombach et al., 2022; Peebles & Xie, 2023; Bao et al., 2023; Chen et al., 2024a; Xie et al., 2023; Wu et al., 2023a; Lipman et al., 2022; Xie et al., 2025a; Qin et al., 2025; Zhang et al., 2023; Seawead et al., 2025). Despite these remarkable capabilities, existing methods suffer from a critical limitation: an overwhelming reliance on English as the primary—and often exclusive—input language (Ramesh et al., 2022; Xie et al., 2025b; Chameleon Team, 2024). This monolingual bias creates substantial barriers for the billions of users who communicate in other languages, fundamentally restricting global access to state-of-the-art generative AI technologies (Bassignana et al., 2025; Peppin et al., 2025). The consequences of this linguistic limitation extend far beyond mere inconvenience. As text-to-image systems become integral to education, creative industries, art, and journalism, the lack of native multilingual support perpetuates existing digital divides and cultural inequities (Liu et al., 2023; Rege et al., 2025). Non-English speakers are forced to navigate through translation layers that not only introduce friction but also risk losing the nuanced meanings and cultural contexts that make their creative expressions unique (Kannen et al., 2024; Friedrich et al., 2024). Building truly multilingual models, like we do in this paper, is therefore not merely a technical challenge but an ethical imperative, one that ensures equitable access to generative AI while preserving linguistic diversity and cultural authenticity in the digital age.

Existing approaches to multilingual image generation typically employ a translation-first strategy, converting non-English prompts to English before processing. While this appears pragmatic, it introduces a cascade of problems that fundamentally compromise the user experience (Kreutzer et al., 2025; Li et al., 2025b; Bafna et al., 2025). The computational overhead of chaining translation and generation models effectively doubles inference time, creating prohibitive delays for real-time applications, thereby further disadvantaging non-English speakers. Most critically, this approach suffers from semantic drift—the systematic loss of culturally specific meanings and linguistic subtleties (Cohn-Gordon & Goodman, 2019; Vanmassenhove et al., 2019; Beinborn & Choenni, 2020). For instance consider the Dutch term “*gezellig*” which encompasses a complex blend of coziness, conviviality, and belonging and has no direct English equivalent. When forced through translation, such rich cultural concepts are inevitably flattened or distorted, resulting in generated images that

054
055
056
057
058
059
060
061
062
063
064
065
066
067
068
069
070
071
072
073
074
075
076
077
078
079
080
081
082
083
084
085
086
087
088
089
090
091
092
093
094
095
096
097
098
099
100
101
102
103
104
105
106
107

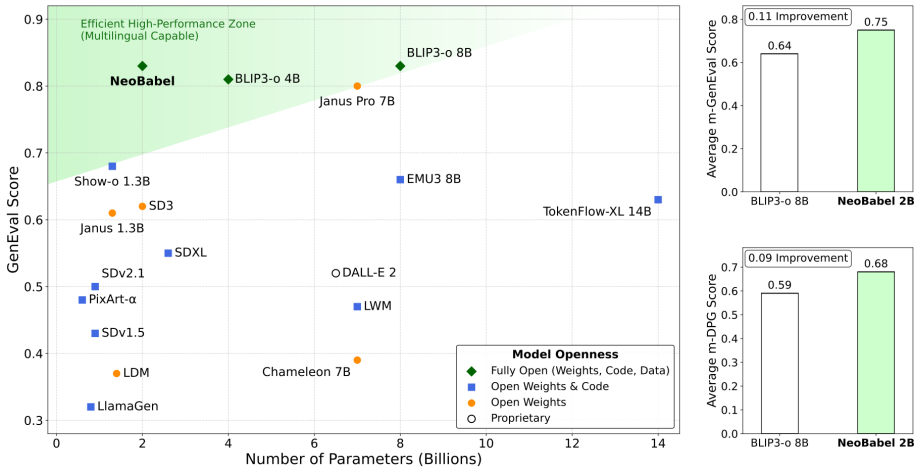


Figure 1: **NeoBabel establishes a new Pareto frontier in multilingual image generation performance, efficiency, and inclusivity.** Left: GenEval English-only scores show that NEOBABEL matches state-of-the-art models despite being 2–4× smaller. Right: On our multilingual benchmark extensions, m-GenEval and m-DPG, NEOBABEL outperforms the second-best model, demonstrating strong multilingual generalization. NEOBABEL is fully open (weights, code, data) and supports six languages with consistent cross-lingual performance.

fail to capture the intended meaning. The fundamental issue lies deeper than mere translation accuracy (Wein & Schneider, 2023; Singh et al., 2024; Salazar et al., 2025). We bypass this limitation by leveraging the image directly. We first caption an image in a target language (English) and then translate this English caption into other languages. The subsequent translations are image-grounded, as they are based on a description generated from the visual input itself.

This paper introduces NEOBABEL, a novel multilingual image generation framework that represents the first scalable solution for direct text-to-image synthesis across six languages: *English, Chinese, Dutch, French, Hindi, and Persian*. It achieves language-agnostic understanding without requiring translation, while maintaining performance parity that matches or exceeds English-only models across all languages (Figure 1). The NEOBABEL architecture delivers operational efficiency, processing multilingual prompts 2.8x faster than ‘translation-then-generation’ pipelines while using 59% less memory which is critical for real-world deployment scenarios (Section 2). To train the model, we introduce a data curation pipeline that prepares 124M multilingual image-text pairs (Section 3) for both pretraining and instruction tuning through progressive training stages (Section 4). We further introduce the first standardized framework for evaluating multilingual image generation, addressing critical gaps in existing benchmarks (Section 5). Our protocol includes: (1) extended versions of GenEval (Ghosh et al., 2023) and DPG-Bench (Hu et al., 2024), referred to as m-GenEval and m-DPG, across six languages, enabling direct comparison between native multilingual and translation-based approaches (Section 6). Finally, we release a comprehensive research toolkit comprising NEOBABEL model checkpoints trained on six languages, a systematically curated dataset of 124M multilingual text-image pairs with quality-controlled translations, and a complete reproducibility package including training scripts, hyperparameter configurations, and standardized evaluation protocols.

2 NEOBABEL ARCHITECTURE

Our architecture’s core components, a multilingual tokenizer and transformer backbone, are optimized for efficient, scalable cross-lingual image generation, supporting seamless processing across diverse languages and image types. Figure 2 provides an overview of the NEOBABEL architecture.

Tokenizers. For textual input, we adopt the multilingual tokenizer of Gemma-2 (Gemma Team et al., 2024) without any modifications. This approach maintains compatibility with multilingual inputs while utilizing proven tokenization methods from language modeling. For image input, we leverage the MAGVIT-v2 quantizer (Yu et al., 2023) retrained by Show-o (Xie et al., 2025b) on 25 million images. This lookup-free quantizer learns a discrete codebook of size $K=8,192$ and encodes

108
109
110
111
112
113
114
115
116
117
118
119
120
121
122
123
124
125
126
127
128
129
130
131
132
133
134
135
136
137
138
139
140
141
142
143
144
145
146
147
148
149
150
151
152
153
154
155
156
157
158
159
160
161

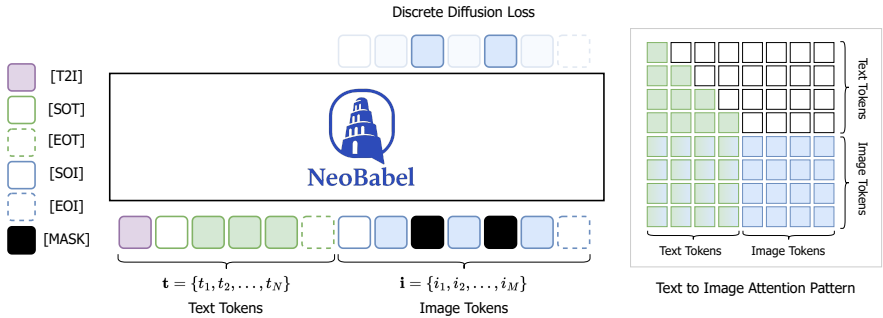


Figure 2: **NeoBabel architecture.** Regardless of modality, all input data is first tokenized and embedded into a unified input sequence. NEOBABEL then applies causal attention to text tokens and full attention within a discrete denoising diffusion framework for image tokens, ultimately generating the desired image.

256 × 256 resolution images into 16 × 16 grids of discrete tokens. The quantization approach supports efficient downstream training and generation while preserving fine-grained visual details.

Transformer Backbone. As we build upon the pretrained multilingual large language model (LLM) Gemma-2 (Gemma Team et al., 2024), we maintain its overall transformer architecture, while introducing two key modifications: (1) integration of a unified multimodal embedding space, and (2) modality-aware attention patterns for flexible generation. Additionally, we apply qk-norm (Henry et al., 2020) to each attention layer to enhance training stability and convergence.

Unified Multimodal Embedding and Prompt Design. To enable seamless multimodal learning, we extend the LLM’s embedding table with 8,192 new learnable embeddings for discrete image tokens, allowing the model to process image inputs natively without architectural changes. Both text and image tokens are embedded in a shared space, enabling the model to learn cross-modal compositionality and semantic alignment. We represent all tasks including text-to-image generation as unified autoregressive sequences. Given a tokenized image-text pair, text and image tokens are concatenated into a single sequence. Special tokens such as [T2I], [SOT], [EOT], [SOI], and [EOI] explicitly mark task type and modality boundaries, enabling the model to disambiguate different modalities and tasks through prompting alone. This design simplifies the training pipeline by removing the need for modality-specific components or task-specific heads, allowing for flexible, scalable, and unified multimodal generation.

Modality-Aware Attention. To accommodate differing structural needs of text and image modalities, we employ a hybrid attention mechanism. Text tokens are modeled with causal attention to preserve autoregressive language modeling capabilities. Image tokens are modeled using full bidirectional attention, allowing rich interactions critical for high-fidelity image synthesis. When both modalities are present, attention masks are dynamically configured so that image tokens can fully attend to text tokens and preceding image tokens, enabling coherent, contextually grounded generation.

Training Objective. The model is trained on sequences composed of both textual and visual tokens, where text tokens act as a prefix and visual tokens form the postfix. We do not apply any learning objective to the text tokens; the loss is computed solely over the visual tokens. Let $\mathbf{t} = \{t_1, t_2, \dots, t_N\}$ denote the text tokens and $\mathbf{i} = \{i_1, i_2, \dots, i_M\}$ denote the image tokens, forming a full input sequence $[\mathbf{t}; \mathbf{i}]$. During training, we randomly select a subset $\mathcal{J} \subset \{1, \dots, M\}$ of image token indices to be masked. The corresponding masked sequence is denoted by \mathbf{i}_* , where i_j is replaced with a special [MASK] token for all $j \in \mathcal{J}$. The model is trained to reconstruct the original visual tokens at the masked positions by conditioning on the full input sequence of text tokens and (partially masked) image tokens. The objective is defined as: $\mathcal{L} = \sum_{j \in \mathcal{J}} \log p_{\theta}(i_j | \mathbf{t}, \mathbf{i}_*)$, where $p_{\theta}(\cdot)$ is the model’s predicted distribution over image codebook entries, parameterized by θ . The loss is only applied to the masked image tokens in \mathcal{J} . We randomly mask a fixed ratio of visual tokens within each training sample (Xie et al., 2025b). To further improve generation controllability, we incorporate classifier-free guidance (Ho & Salimans, 2022) by replacing the conditioning text with a null string with some probability during training.

Table 1: **NeoBabel multilingual datasets**, detailing their English-only data source, image origin, caption format, and size. Our multilingual expansion covers model-generated recaptioning, translation into multiple languages, or both and increase the total size from 39M to 124M image-caption/label pairs. All modified datasets are prefixed with m- to denote their expanded form.

Original English-Only Dataset				NEOBABEL Multilingual Expansion		
Dataset	Image Source	Caption Source	Size	Recaptioning	Translation	New Size
ImageNet 1K	Web	Class labels	1M	–	✓	6M
CC12M	Web	Alt-text (noisy)	12M	✓	–	12M
SA-1B	Photography	LLaVA	10M	✓	–	10M
LAION-Aesthetic	Web	Alt-text (noisy)	12M	✓	✓	72M
JourneyDB	Synthetic	GPT-3.5	4M	✓	✓	24M
BLIP3-o Instruct	Web + Synthetic	GPT-4o / human	60K	–	✓	360K
			39M			124M

3 NEOBABEL MULTILINGUAL DATASETS

Data curation pipeline. Multilingual multimodal data remains scarce, especially compared to the abundance of English-centric resources. This imbalance poses a significant barrier to training and evaluating models that can understand grounded language across diverse linguistic contexts. To address this gap, we curate and augment several multilingual datasets by translating and recaptioning existing image-caption pairs into six target languages: *English*, *Chinese*¹, *Dutch*, *French*, *Hindi*, and *Persian*. We summarize the datasets curated in Table 1. At the core of our approach is a multilingual captioning pipeline designed to ensure both semantic richness and linguistic diversity. We begin by generating a detailed English caption for each image using InternVL (Chen et al., 2024c), prompted with a simple instruction: “Describe this image in detail in English.” This step guarantees comprehensive coverage of the visual content. To preserve quality and consistency across languages, we apply length filtering, language validation, visual-text mismatch and toxicity/NSFW filterings, with full details provided in Appendix A.5. Once high-quality English captions are obtained, we translate them into five target languages using the NLLB model (Costa-Jussà et al., 2022) for the pretraining datasets, and the Gemini Experimental model (gemini-2.0-flash-lite) for the instruction tuning datasets. Ultimately, this step plays a central role in constructing a high-quality, language-balanced multimodal resource, essential for more inclusive and globally-relevant vision-language models.

NEOBABEL pretraining data. We use a diverse collection of image-text datasets to build strong multilingual visual-language alignment combining real-world and synthetic image sources. While the images are drawn from established, high-quality datasets, the accompanying captions have been significantly enriched through our recaptioning and multilingual translation pipeline resulting in a more diverse, detailed, and valuable resource. The original English class labels are translated into five additional languages to obtain a total of six target languages, forming multilingual textual prompts for class-conditional image generation, denoted as *m-ImageNet-1K*. We further incorporate *m-SA-1B* and *m-CC12M*, consisting of 22 million English image-caption pairs (Kirillov et al., 2023; Changpinyo et al., 2021), which provide rich natural descriptions and enhance visual diversity; their texts are refined through our recaptioning pipeline. In addition, *m-LAION-Aesthetic*, a 12M subset of the LAION dataset (Clure, 2023), is enhanced and translated, yielding approximately 72 million image-caption pairs across six languages. Finally, *m-JourneyDB*, a synthetic dataset of 4 million high-quality Midjourney-generated images (Sun et al., 2023a), is processed with the same recaptioning and translation pipeline, resulting in 24 million multilingual pairs. Combining all sources, the final pretraining dataset contains approximately 124 million image-text pairs spanning six languages, covering diverse domains and visual aesthetics.

NEOBABEL instruction tuning data. We describe the datasets and mixing strategies used for instruction tuning. This phase reuses two datasets introduced earlier and adds a smaller but higher-quality dataset focused on multimodal supervision. Specifically, we continue to use *m-LAION-Aesthetic* and *m-JourneyDB*, as extended in the pretraining stage, and introduce *m-BLIP3o-Instruct*, an instruction-focused dataset from Chen et al. (2025a) containing multimodal instruction samples translated into six languages for multilingual training. All images are resized to 512×512 . While

¹Throughout this work ‘Chinese’ refers to Simplified Chinese.

the images are drawn from established, high-quality sources, most accompanying texts have been enriched or rewritten, resulting in a more valuable and linguistically diverse dataset.

4 NEOBABEL TRAINING STAGES: LEARNING PROGRESSION

NEOBABEL is trained using a staged learning framework consisting of three progressive pretraining stages followed by two instruction tuning stages. Training details are provided in Appendix A.2.

Progressive pretraining. Our pretraining progressively scales from basic visual understanding to advanced multilingual image generation. In [Stage 1 \(Pixel Dependency Learning\)](#), the model learns foundational visual representations using m-ImageNet-1K, where class-conditional generation is guided by translated class labels to capture pixel-level dependencies and build robust image token embeddings. [Stage 2 \(Scaling Alignment with Large-Scale Multilingual Data\)](#) fine-tunes the model on 22 million English-only image-caption pairs from m-SA-1B and m-CC12M, together with 72 million translated samples from m-LAION-Aesthetic, strengthening natural image-text alignment and expanding multilingual capabilities through broad cross-lingual exposure. Finally, [Stage 3 \(Refined Multilingual Pretraining\)](#) trains on 96 million multilingual pairs from m-LAION-Aesthetic and m-JourneyDB, balancing high-quality real-world aesthetic data with diverse synthetic images to enhance generalization across languages, domains, and modalities.

Progressive instruction tuning. In this phase, the model focuses on explicit task-guided adaptation, refining its ability to interpret and execute complex, multilingual instructions through our curated datasets and progressive exposure to prompt-driven generation in two stages. [Stage 1 \(Initial Multilingual Instruction Alignment\)](#) trains the model with a diverse mixture of m-LAION-Aesthetic, m-JourneyDB, and m-BLIP3o-Instruct using mixing weights α_1 , α_2 , and α_3 such that $\alpha_1 + \alpha_2 + \alpha_3 = 100$. A higher α_1 and moderate α_2 prioritize real-world and aesthetic content, while a smaller α_3 introduces early exposure to instruction-rich samples, helping the model learn cross-lingual, cross-modal grounding without being overwhelmed by complex prompts. In [Stage 2 \(Instruction Refinement\)](#), the mixing weights are shifted to emphasize instruction-rich and synthetic supervision by increasing α_2 and α_3 and reducing α_1 , enabling the model to refine its multilingual instruction-following abilities through complex prompts and high-quality synthetic images. This curriculum-style adjustment increases semantic richness and improves generalization to both benchmark instruction tasks and open-ended generation scenarios.

5 MULTILINGUAL EVALUATION OF IMAGE GENERATION

Existing image generation benchmarks are mostly English-centric, failing to capture cross-lingual performance. We introduce a multilingual evaluation suite that extends established (English-only) benchmarks to cover six diverse languages. We assess the image generation capabilities of NEOBABEL using two complementary benchmarks: GenEval ([Ghosh et al., 2023](#)) and DPG-Bench ([Hu et al., 2024](#)). GenEval offers a structured evaluation of prompt-to-image alignment across six compositional dimensions: *single object*, *two objects*, *counting*, *colors*, *position*, and *color attribute*. In contrast, DPG-Bench targets general-purpose generation with open-ended, diverse prompts that test broader semantic understanding. However, both benchmarks are English-only and fail to capture multilingual generative performance. As part of our multilingual evaluation suite, we introduce **m-GenEval** and **m-DPG**, multilingual extensions of the original benchmarks. All prompts are translated into five additional languages: *Chinese*, *Dutch*, *French*, *Hindi*, and *Persian*, using the Gemini Experimental model, followed by human verification and manual corrections to ensure linguistic correctness. We also publicly release m-GenEval and m-DPG to promote inclusive and realistic evaluation of multilingual text-to-image models and support broader community adoption.

6 RESULTS AND DISCUSSIONS

6.1 MULTILINGUAL IMAGE GENERATION PERFORMANCE

m-GenEval Comparison. We evaluate NEOBABEL on the English prompts of the m-GenEval benchmark, with results reported in Table 2. The comparison includes both generative models (G), which focus solely on text-to-image generation, and unified models (U&G), which also support image understanding tasks such as captioning and visual question answering. Despite having only 2B parameters, NEOBABEL outperforms or matches best-performing unified models such as Janus-Pro 7B (0.80) and BLIP3-o 8B (0.83), which are larger in terms of parameters. It also surpasses SD3

Table 2: **English-only GenEval benchmark comparison.** NEOBABEL achieves the highest overall score, outperforming larger models on tasks requiring compositional reasoning and fine-grained prompt-image alignment. Symbol legend: \oplus denotes multilingual generation capability, with \checkmark indicates a full multilingual capability, \circ represents partial multilingual capability (i.e. bilingual or multilingual to a limited extent), and \times denotes monolingual models.

Method	\oplus	Type	Params.	Single Object	Two Object	Counting	Colors	Position	Color Attribute	Overall
LlamaGen	\times	G	0.8B	0.71	0.34	0.21	0.58	0.07	0.04	0.32
PixArt-alpha	\times	G	0.6B	0.98	0.50	0.44	0.80	0.08	0.07	0.48
SDXL	\times	G	2.6B	0.98	0.74	0.39	0.85	0.15	0.23	0.55
SD3	\times	G	2B	0.98	0.74	0.63	0.67	0.34	0.36	0.62
Chameleon	\times	U&G	7B	-	-	-	-	-	-	0.39
LWM	\circ	U&G	7B	0.93	0.41	0.46	0.79	0.09	0.15	0.47
TokenFlow	\circ	U&G	14B	-	-	-	-	-	-	0.63
EMU3	\circ	U&G	8B	-	-	-	-	-	-	0.66
Show-o	\times	U&G	1.3B	0.98	0.80	0.66	0.84	0.31	0.50	0.68
Janus-Pro	\circ	U&G	7B	-	-	-	-	-	-	0.80
BLIP3-o	\circ	U&G	4B	-	-	-	-	-	-	0.81
BLIP3-o	\circ	U&G	8B	-	-	-	-	-	-	0.83
NEOBABEL	\checkmark	G	2B	1.00	0.91	0.62	0.91	0.81	0.77	0.83

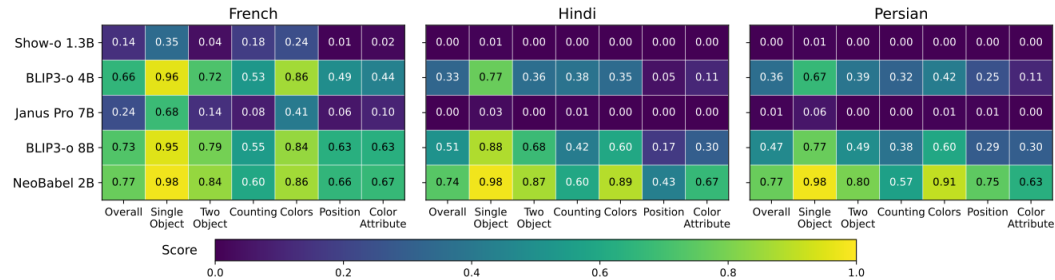


Figure 3: **m-GenEval benchmark comparison.** Models such as Janus Pro and BLIP3-o drop sharply in non-English settings, while NEOBABEL delivers consistent performance across languages (see Figure 10 in the appendix for all six languages).

2B (0.62), a leading model in the generative category, achieving the highest overall score of 0.83. This performance reflects strong fine-grained and compositional prompt-image alignment particularly in challenging subcategories like color attributes and positional grounding. In Figure 3, we report results on a representative subset of three languages, where NEOBABEL surpasses baselines in medium-resource French (0.04) and shows large gains in low-resource Hindi and Persian (up to 0.3). The full evaluation across six languages, provided in Figure 10 in the appendix, further reveals only a small gap in high-resource Chinese (0.03) and a moderate one in Dutch (0.06), highlighting the general trend that the advantage of NEOBABEL grows as resource availability decreases.

m-DPG Comparison. We evaluate NEOBABEL on m-DPG (Table 3), which measures semantic accuracy, detail, and coherence. With only 2B parameters, NEOBABEL provides moderate performance on English (0.75) compared to larger models i.e. BLIP3-o (8B) and Janus Pro (7B), while outperforming them in other languages. A consistent trend emerges: in medium-resource languages, the performance gap widens (e.g., +0.10 in Dutch, +0.09 in French), and in low-resource settings it broadens further (+0.13 in Hindi, +0.12 in Persian). This mirrors the pattern observed in m-GenEval, further underscoring the robustness of NEOBABEL in multilingual, low-resource scenarios.

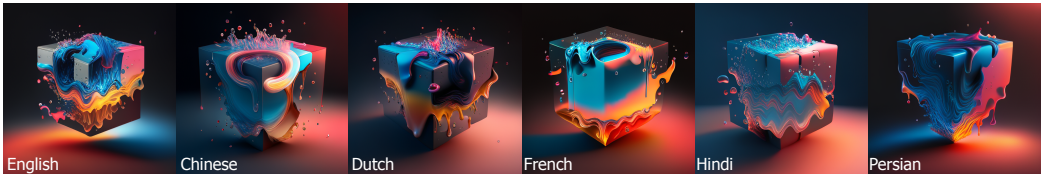
6.2 QUALITATIVE EVALUATION

Multilingual text-to-image generation. We present qualitative results from NEOBABEL across diverse prompt categories, including compositional scenes, abstract concepts, and multilingual instructions. Examples are in Figure 4, with more in Figures 12 and 13 (appendix). As observed, objects, layouts, and attributes are preserved across languages. The results show that NEOBABEL consistently produces semantically aligned and visually coherent images.

Table 3: **m-DPG benchmark comparison.** Despite its small parameter count, NEOBABEL achieves competitive results in English and consistently outperforms all baselines across five non-English languages, demonstrating strong cross-lingual prompt understanding and image generation.

Model	Params.	English	Chinese	Dutch	French	Hindi	Persian	Overall
Show-o	1.3B	0.67	0.10	0.22	0.32	0.04	0.04	0.23
Janus Pro	7B	0.84	0.50	0.61	0.68	0.12	0.12	0.47
BLIP3-o	4B	0.79	0.60	0.58	0.59	0.47	0.49	0.58
BLIP3-o	8B	0.80	0.56	0.59	0.61	0.50	0.53	0.59
NEOBABEL	2B	0.75	0.70	0.69	0.70	0.63	0.65	0.68

English: The image depicts a dynamic and vibrant scene featuring an abstract, three-dimensional cube suspended against a dark background with subtle red hues at the bottom edge. The cube is composed of fluid-like material that appears to be melting into various colors such as blue, pink, orange, yellow, and hints of purple. The liquid forms swirls around its edges like waves crashing over it, creating a sense of motion and energy within the composition. Bubbles are scattered throughout both inside and outside the cube's surface, adding texture and depth to the visual effect. The top part of the cube has more intense shades of blue while transitioning smoothly towards warmer tones on one side, giving off a fiery appearance where bright pinks and yellows dominate. This contrast creates a striking interplay between cool and warm colors across different sections of the object. Light reflections highlight some parts making them appear glossy and wet, enhancing the illusion of movement through light refraction effects visible along the curves formed by the flowing substance.



Chinese: 这张图描绘了一只迷人的动画猫角色，拥有大大的绿色眼睛和富有表现力的面孔，展现出自信与好奇心。猫咪戴着一顶精致的棕色帽子，帽侧装饰有螺丝和别针等配件。它身穿精致的服装，包括一件时尚的马甲，里面似乎是一件浅色衬衫。其毛发图案在耳朵和后腿周围有橙色斑点，赋予它独特的外观。背景为白色，突出了明亮复杂的颜色、衣服的细节和角色面部的表现。尾巴轻轻地弯在身后。整体上，这个设计很好地传达了大胆和好奇的感觉。



Figure 4: **Qualitative evaluation of NEOBABEL.** Each row is based on a single concept expressed in six different languages. We show only one of the prompts (in one language) and present six images generated from its translated prompts in the other five languages. Across all languages, NEOBABEL delivers semantically accurate and visually cohesive outputs with reliable consistency.

Multilingual image inpainting and extrapolation. NEOBABEL supports text-guided image inpainting and extrapolation across languages without additional fine-tuning. This enables collaborative applications, such as a multilingual visual canvas where users contribute prompts in their native languages to co-create expressive scenes. As shown in Figures 14 and 15, NEOBABEL can modify or extend an input image based on prompts in different languages, producing images that remain semantically faithful and visually consistent with the adjacent visual content, highlighting its potential for interactive and multilingual visual editing.



Figure 5: **Multilingual image inpainting.** NEOBABEL supports multilingual text-guided image inpainting, highlighting its potential for interactive visual editing across diverse user groups.

6.3 ABLATIONS AND ANALYSES

Effect of progressive pretraining. We analyze the impact of our progressive pretraining strategy across three stages at 256×256 resolution. Progressive pretraining steadily improves multilingual performance (Figure 7; full results in Figure 11 in the appendix). In stage one, training on m-

378
379
380
381
382
383
384
385
386
387
388
389
390
391
392
393
394
395
396
397
398
399
400
401
402
403
404
405
406
407
408
409
410
411
412
413
414
415
416
417
418
419
420
421
422
423
424
425
426
427
428
429
430
431

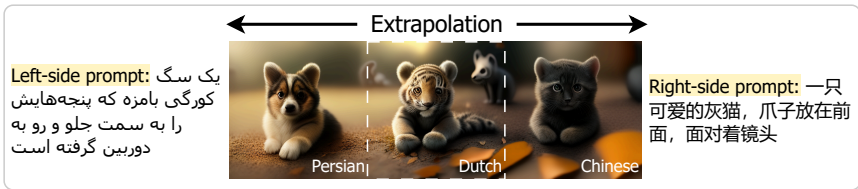


Figure 6: **Multilingual image extrapolation.** NEOBABEL performs text-guided image extrapolation, generating coherent left and right extensions from different multilingual prompts.

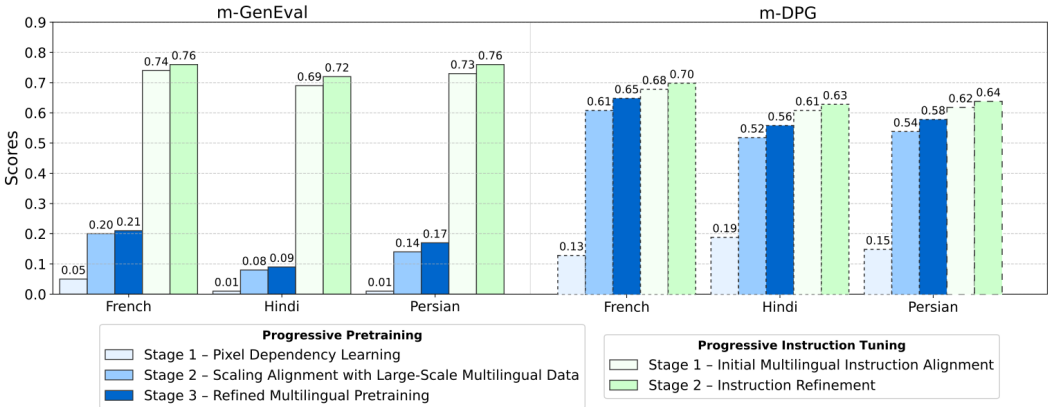


Figure 7: **Effect of progressive pretraining and instruction tuning.** Performance on m-GenEval (left) and m-DPG (right) improves steadily across pretraining and instruction tuning stages. See figure 11 in appendix for results of all six languages on both benchmarks.

ImageNet 1K produces modest scores, reflecting weak multilingual alignment. In stage two, the addition of large but noisy datasets (m-SA-1B, m-CC12M, m-LAION-Aesthetic) drives a significant increase, with gains larger on m-DPG than on m-GenEval, suggesting improved handling of natural multilingual prompts. Stage three incorporates higher-quality datasets (m-LAION-Aesthetic, m-JourneyDB), leading to further improvements. These results highlight the cumulative benefits of progressively increasing both dataset diversity and quality.

Effect of progressive instruction tuning. We analyze the effect of high-resolution instruction tuning at 512×512 resolution using a fixed dataset mixture of m-LAION-Aesthetic, m-JourneyDB, and m-BLIP3o-Instruct. Results are shown in Figure 7, with the full evaluation provided in Figure 11 in the appendix. In the first stage, each training batch consists of 60% m-LAION-Aesthetic, 30% m-JourneyDB, and 10% m-BLIP3o-Instruct samples. This stage yields a substantial multilingual gain on m-GenEval and m-DPG compared to the final stage of pretraining. In the second stage, each training batch shifts emphasis toward higher-quality and instruction-aligned data, consisting of 25% m-LAION-Aesthetic, 60% m-JourneyDB, and 15% m-BLIP3o-Instruct samples. This leads to further multilingual gains in m-GenEval and m-DPG. These results show that beyond increasing the resolution, the relative weight of curated and instruction-focused datasets plays a pivotal role in shaping multilingual capability.

Cross-lingual image generation. A more challenging evaluation of the model’s multilingual capability involves prompts that combine multiple languages within the same input. This requires the model to integrate information from different languages into a coherent and semantically accurate image. To test this, we design cross-lingual prompts by splitting a base prompt into three parts and translating each into a different language. As seen in Figure 16, these results highlight the model’s cross-lingual alignment, despite not being explicitly trained for this task. To further assess robustness, we introduce the Code-Switching Similarity (CSS) score, which measures visual consistency under intra-prompt language variation. We find that NEOBABEL maintains stable performance when language segments are swapped (see Section A.6 in the appendix for details).

432
433
434
435
436
437
438
439
440
441
442
443
444
445
446
447
448
449
450
451
452
453
454
455
456
457
458
459
460
461
462
463
464
465
466
467
468
469
470
471
472
473
474
475
476
477
478
479
480
481
482
483
484
485

Multilingual Input Prompt: A close-up photograph of a Corgi dog. De hond draagt een zwarte hoed en een ronde, donkere zonnebril. Le Corgi a une expression joyeuse, avec la bouche ouverte et la langue tirée, donnant une impression de bonheur ou d'excitation.

English Translation: A close-up photograph of a Corgi dog. The dog is wearing a black hat and round, dark sunglasses. The Corgi has a joyful expression, with its mouth open and tongue sticking out, giving an impression of happiness or excitement.



Figure 8: **Cross-Lingual Prompt Generation.** An example of a code-switched prompt combining English, Dutch, and French, with the image generated by NEOBABEL. English translations are shown for reader convenience, they are not used as input.

7 RELATED WORKS

Visual generative models. Two dominant paradigms have emerged for image and video generation: diffusion-based (Rombach et al., 2022; Ramesh et al., 2022; Peebles & Xie, 2023; Bao et al., 2023; Chen et al., 2024a; Xie et al., 2023; Wu et al., 2023a; Lipman et al., 2022; Xie et al., 2025a; Qin et al., 2025; Zhang et al., 2023; Seawead et al., 2025) and autoregressive (Sun et al., 2024; Kondratyuk et al., 2023; Chen et al., 2020; Pang et al., 2024; Li et al., 2025a) models. Diffusion models typically combine pretrained text encoders with denoising networks to iteratively refine visual outputs, while autoregressive models adopt LLM-based architectures trained via next-token prediction. Recent hybrid approaches (Li et al., 2024b; Liu et al., 2024b; Fan et al., 2025) attempt to unify the strengths of both paradigms for more powerful generation. NEOBABEL follows the diffusion-based paradigm but distinguishes itself by adopting an LLM-style architecture for visual token modeling. This removes the reliance on frozen text encoders and instead builds on top of a strong multilingual decoder-based LLM, enabling tighter integration between language and vision.

Unified multimodal models. Unified multimodal models aim to handle both image understanding and generation within a single architecture, typically categorized into native and adapter-based approaches. Native approaches such as Chameleon (Chameleon Team, 2024), Show-o (Xie et al., 2025b), Transfusion (Zhou et al., 2025), and Janus (Wu et al., 2025) adopt either autoregressive, diffusion, or hybrid modeling strategies to jointly process vision and language. Recent work (Wang et al., 2024; Wu et al., 2024; Ma et al., 2025; Jiao et al., 2025; Chen et al., 2025b; Song et al., 2025) has focused on improving tokenization and training efficiency to enhance cross-modal alignment. A parallel direction (Tang et al., 2023; Lu et al., 2023; Dong et al., 2024; Ge et al., 2024; Tong et al., 2024; Pan et al., 2025; Chen et al., 2025a; Wu et al., 2023b) constructs unified multimodal models by connecting pretrained LMMs and generative models via adapters or learnable tokens. While modular and flexible, these systems often rely on frozen components and lack full cross-modal integration. Our model, NEOBABEL, aligns more closely with native unified multimodal models by unifying visual and textual modeling within a single decoder-based architecture, without relying on adapters or frozen backbones. Although NEOBABEL supports multilingual multimodal understanding, this work focuses specifically on multilingual image generation.

8 CONCLUSION

NEOBABEL demonstrates that high-quality, efficient multilingual image generation is not only possible but also advantageous. Through strategic data curation and a unified architecture, we set a new Pareto frontier in performance, efficiency, and inclusivity.

Limitations. While NEOBABEL demonstrates strong multilingual image generation capabilities, several limitations remain. First, the model currently supports six languages; extending to broader linguistic coverage would require tokenizer adaptation and additional training. Second, although NEOBABEL adopts a unified architecture, it does not yet support vision-language tasks such as visual question answering, due to the absence of task-specific fine-tuning. We leave these directions, including task expansion, larger-scale scaling, and broader language coverage, for future research.

Future work. This work contributes to the broader goal of democratizing generative AI. By releasing all model weights, datasets, and evaluation protocols, we aim to encourage the research community to build upon this foundation, ultimately advancing toward generative models that better reflect and serve global linguistic and cultural diversity.

486 **Ethics statement.** All experiments are conducted on *publicly available* datasets used under their
487 original licenses, without collecting new human data or personal annotations. Although the model
488 is not designed to predict demographics or sensitive traits, it may reflect biases in the training data
489 and could be misapplied to privacy-invasive or unauthorized tasks. We caution against such uses and
490 highlight the importance of following license terms, governance standards, and legal requirements.

491 **Reproducibility statement.** All models, datasets, and baselines in this work are publicly avail-
492 able. We detail training and validation splits, optimization settings, and evaluation protocols in the
493 main text, with further implementation specifics in the appendix. To support replication, we release
494 the full pipeline covering data curation, pretraining, instruction tuning, and evaluation. Training
495 was performed in distributed setups using either 8×NVIDIA H100 (80GB) or 16×AMD MI250x
496 (128GB) GPUs.

499 REFERENCES

501 Nahid Alam, Karthik Reddy Kanjula, Surya Guthikonda, Timothy Chung, Bala Krishna S Vegesna,
502 Abhipsha Das, Anthony Susevski, Ryan Sze-Yin Chan, SM Uddin, Shayekh Bin Islam, et al. Maya: An instruction finetuned multilingual multimodal model. *arXiv preprint arXiv:2412.07112*, 2024.

505 Nahid Alam, Karthik Reddy Kanjula, Surya Guthikonda, Timothy Chung, Bala Krishna S Vegesna,
506 Abhipsha Das, Anthony Susevski, Ryan Sze-Yin Chan, SM Uddin, Shayekh Bin Islam, et al. Behind maya: Building a multilingual vision language model. *arXiv preprint arXiv:2505.08910*, 2025.

509 Niyati Bafna, Tianjian Li, Kenton Murray, David R Mortensen, David Yarowsky, Hale Sirin, and
510 Daniel Khashabi. The translation barrier hypothesis: Multilingual generation with large language
511 models suffers from implicit translation failure. *arXiv preprint arXiv:2506.22724*, 2025.

513 Shuai Bai, Keqin Chen, Xuejing Liu, Jialin Wang, Wenbin Ge, Sibao Song, Kai Dang, Peng Wang,
514 Shijie Wang, Jun Tang, Humen Zhong, Yanzhi Zhu, Mingkun Yang, Zhaohai Li, Jianqiang Wan,
515 Pengfei Wang, Wei Ding, Zheren Fu, Yiheng Xu, Jiabo Ye, Xi Zhang, Tianbao Xie, Zesen Cheng,
516 Hang Zhang, Zhibo Yang, Haiyang Xu, and Junyang Lin. Qwen2.5-vl technical report. *arXiv preprint arXiv:2502.13923*, 2025.

518 Fan Bao, Shen Nie, Kaiwen Xue, Yue Cao, Chongxuan Li, Hang Su, and Jun Zhu. All are worth
519 words: A vit backbone for diffusion models. In *Conference on Computer Vision and Pattern Recognition*, 2023.

522 Elisa Bassignana, Amanda Cercas Curry, and Dirk Hovy. The ai gap: How socioeconomic status
523 affects language technology interactions. *arXiv preprint arXiv:2505.12158*, 2025.

524 Lisa Beinborn and Rochelle Choenni. Semantic drift in multilingual representations. *Computational Linguistics*, 2020.

527 Chameleon Team. Chameleon: Mixed-modal early-fusion foundation models. *arXiv preprint arXiv:2405.09818*, 2024.

529 Soravit Changpinyo, Piyush Sharma, Nan Ding, and Radu Soricut. Conceptual 12m: Pushing web-
530 scale image-text pre-training to recognize long-tail visual concepts. In *Conference on Computer Vision and Pattern Recognition*, 2021.

533 Jiuhai Chen, Zhiyang Xu, Xichen Pan, Yushi Hu, Can Qin, Tom Goldstein, Lifu Huang, Tianyi
534 Zhou, Saining Xie, Silvio Savarese, et al. Blip3-o: A family of fully open unified multimodal
535 models-architecture, training and dataset. *arXiv preprint arXiv:2505.09568*, 2025a.

536
537 Junsong Chen, Jincheng Yu, Chongjian Ge, Lewei Yao, Enze Xie, Zhongdao Wang, James T. Kwok,
538 Ping Luo, Huchuan Lu, and Zhenguo Li. Pixart- α : Fast training of diffusion transformer for
539 photorealistic text-to-image synthesis. In *International Conference on Learning Representations*, 2024a.

- 540 Mark Chen, Alec Radford, Rewon Child, Jeffrey Wu, Heewoo Jun, David Luan, and Ilya Sutskever.
541 Generative pretraining from pixels. In *International Conference on Machine Learning*, 2020.
542
- 543 Zhe Chen, Weiyun Wang, Yue Cao, Yangzhou Liu, Zhangwei Gao, Erfei Cui, Jinguo Zhu, Sheng-
544 long Ye, Hao Tian, Zhaoyang Liu, et al. Expanding performance boundaries of open-source
545 multimodal models with model, data, and test-time scaling. *arXiv preprint arXiv:2412.05271*,
546 2024b.
- 547 Zhe Chen, Jiannan Wu, Wenhai Wang, Weijie Su, Guo Chen, Sen Xing, Muyan Zhong, Qinglong
548 Zhang, Xizhou Zhu, Lewei Lu, et al. Internvl: Scaling up vision foundation models and aligning
549 for generic visual-linguistic tasks. In *Conference on Computer Vision and Pattern Recognition*,
550 2024c.
- 551 Zisheng Chen, Chunwei Wang, Xiuwei Chen, Hang Xu, Jianhua Han, and Xiaodan Liang. Semhi-
552 tok: A unified image tokenizer via semantic-guided hierarchical codebook for multimodal under-
553 standing and generation. *arXiv preprint arXiv:2503.06764*, 2025b.
554
- 555 David Clure. Laion-aesthetics-12m umap dataset. [https://huggingface.co/datasets/
556 dclure/laion-aesthetics-12m-umap](https://huggingface.co/datasets/dclure/laion-aesthetics-12m-umap), 2023. Dataset.
- 557 Reuben Cohn-Gordon and Noah Goodman. Lost in machine translation: A method to reduce mean-
558 ing loss. In Jill Burstein, Christy Doran, and Tamar Solorio (eds.), *Proceedings of the 2019
559 Conference of the North American Chapter of the Association for Computational Linguistics:
560 Human Language Technologies, Volume 1 (Long and Short Papers)*, 2019.
- 561 Marta R Costa-Jussà, James Cross, Onur Çelebi, Maha Elbayad, Kenneth Heafield, Kevin Heffernan,
562 Elahe Kalbassi, Janice Lam, Daniel Licht, Jean Maillard, et al. No language left behind: Scaling
563 human-centered machine translation. *arXiv preprint arXiv:2207.04672*, 2022.
564
- 565 Saurabh Dash, Yiyang Nan, John Dang, Arash Ahmadian, Shivalika Singh, Madeline Smith,
566 Bharat Venkitesh, Vlad Shmyhlo, Viraat Aryabumi, Walter Beller-Morales, Jeremy Pekmez, Ja-
567 son Ozuzu, Pierre Richemond, Acyr Locatelli, Nick Frosst, Phil Blunsom, Aidan Gomez, Ivan
568 Zhang, Marzieh Fadaee, Manoj Govindassamy, Sudip Roy, Matthias Gallé, Beyza Ermis, Ahmet
569 Üstün, and Sara Hooker. Aya vision: Advancing the frontier of multilingual multimodality. *arXiv
570 preprint arXiv:2505.08751*, 2025.
- 571 Matt Deitke, Christopher Clark, Sangho Lee, Rohun Tripathi, Yue Yang, Jae Sung Park, Moham-
572 madreza Salehi, Niklas Muennighoff, Kyle Lo, Luca Soldaini, et al. Molmo and pixmo: Open
573 weights and open data for state-of-the-art multimodal models. In *Conference on Computer Vision
574 and Pattern Recognition*, 2025.
- 575 Haiwen Diao, Yufeng Cui, Xiaotong Li, Yueze Wang, Huchuan Lu, and Xinlong Wang. Unveiling
576 encoder-free vision-language models. *arXiv preprint arXiv:2406.11832*, 2024.
577
- 578 Haiwen Diao, Xiaotong Li, Yufeng Cui, Yueze Wang, Haoge Deng, Ting Pan, Wenxuan Wang,
579 Huchuan Lu, and Xinlong Wang. Evev2: Improved baselines for encoder-free vision-language
580 models. *arXiv preprint arXiv:2502.06788*, 2025.
- 581 Runpei Dong, Chunrui Han, Yuang Peng, Zekun Qi, Zheng Ge, Jinrong Yang, Liang Zhao, Jianjian
582 Sun, Hongyu Zhou, Haoran Wei, Xiangwen Kong, Xiangyu Zhang, Kaisheng Ma, and Li Yi.
583 DreamLLM: Synergistic multimodal comprehension and creation. In *International Conference
584 on Learning Representations*, 2024.
- 585 Lijie Fan, Luming Tang, Siyang Qin, Tianhong Li, Xuan Yang, Siyuan Qiao, Andreas Steiner, Chen
586 Sun, Yuanzhen Li, Tao Zhu, et al. Unified autoregressive visual generation and understanding
587 with continuous tokens. *arXiv preprint arXiv:2503.13436*, 2025.
588
- 589 Felix Friedrich, Katharina Hammerl, Patrick Schramowski, Manuel Brack, Jindrich Libovicky, Kris-
590 tian Kersting, and Alexander Fraser. Multilingual text-to-image generation magnifies gender
591 stereotypes and prompt engineering may not help you. *arXiv preprint arXiv:2401.16092*, 2024.
- 592 Yuying Ge, Sijie Zhao, Jinguo Zhu, Yixiao Ge, Kun Yi, Lin Song, Chen Li, Xiaohan Ding, and Ying
593 Shan. Seed-x: Multimodal models with unified multi-granularity comprehension and generation.
arXiv preprint arXiv:2404.14396, 2024.

- 594 Gemma Team, Morgane Riviere, Shreya Pathak, Pier Giuseppe Sessa, Cassidy Hardin, Surya Bhu-
595 patiraju, Léonard Hussenot, Thomas Mesnard, Bobak Shahriari, Alexandre Ramé, et al. Gemma
596 2: Improving open language models at a practical size. *arXiv preprint arXiv:2408.00118*, 2024.
597
- 598 Dhruva Ghosh, Hannaneh Hajishirzi, and Ludwig Schmidt. Geneval: An object-focused framework
599 for evaluating text-to-image alignment. *Advances on Neural Information Processing Systems*,
600 2023.
- 601 Alex Henry, Prudhvi Raj Dachapally, Shubham Pawar, and Yuxuan Chen. Query-key normalization
602 for transformers. *arXiv preprint arXiv:2010.04245*, 2020.
603
- 604 Jonathan Ho and Tim Salimans. Classifier-free diffusion guidance. *arXiv preprint*
605 *arXiv:2207.12598*, 2022.
- 606 Xiwei Hu, Rui Wang, Yixiao Fang, Bin Fu, Pei Cheng, and Gang Yu. Ella: Equip diffusion models
607 with llm for enhanced semantic alignment. *arXiv preprint arXiv:2403.05135*, 2024.
608
- 609 Yang Jiao, Haibo Qiu, Zequn Jie, Shaoxiang Chen, Jingjing Chen, Lin Ma, and Yu-Gang Jiang. Uni-
610 token: Harmonizing multimodal understanding and generation through unified visual encoding.
611 *arXiv preprint arXiv:2504.04423*, 2025.
- 612 Armand Joulin, Edouard Grave, Piotr Bojanowski, Matthijs Douze, Herve Jégou, and Tomas
613 Mikolov. Fasttext.zip: Compressing text classification models. *arXiv preprint arXiv:1612.03651*,
614 2016.
- 615 Nithish Kannen, Arif Ahmad, marco Andreetto, Vinodkumar Prabhakaran, Utsav Prabhu,
616 Adji Bousso Dieng, Pushpak Bhattacharyya, and Shachi Dave. Beyond aesthetics: Cultural compe-
617 tence in text-to-image models, 2024.
618
- 619 Alexander Kirillov, Eric Mintun, Nikhila Ravi, Hanzi Mao, Chloe Rolland, Laura Gustafson, Tete
620 Xiao, Spencer Whitehead, Alexander C Berg, Wan-Yen Lo, et al. Segment anything. In *IEEE*
621 *International Conference on Computer Vision*, 2023.
- 622 Dan Kondratyuk, Lijun Yu, Xiuye Gu, José Lezama, Jonathan Huang, Rachel Hornung, Hartwig
623 Adam, Hassan Akbari, Yair Alon, Vighnesh Birodkar, et al. Videopoet: A large language model
624 for zero-shot video generation. *arXiv preprint arXiv:2312.14125*, 2023.
625
- 626 Julia Kreutzer, Eleftheria Briakou, Sweta Agrawal, Marzieh Fadaee, and Kocmi Tom. Déjà vu:
627 Multilingual llm evaluation through the lens of machine translation evaluation, 2025.
- 628 Woosuk Kwon, Zhuohan Li, Siyuan Zhuang, Ying Sheng, Lianmin Zheng, Cody Hao Yu, Joseph E.
629 Gonzalez, Hao Zhang, and Ion Stoica. Efficient memory management for large language model
630 serving with pagedattention. In *Proceedings of the ACM SIGOPS 29th Symposium on Operating*
631 *Systems Principles*, 2023.
- 632 Bo Li, Yuanhan Zhang, Dong Guo, Renrui Zhang, Feng Li, Hao Zhang, Kaichen Zhang, Yanwei
633 Li, Ziwei Liu, and Chunyuan Li. Llava-onevision: Easy visual task transfer. *arXiv preprint*
634 *arXiv:2408.03326*, 2024a.
635
- 636 Haopeng Li, Jinyue Yang, Guoqi Li, and Huan Wang. Autoregressive image generation with ran-
637 domized parallel decoding. *arXiv preprint arXiv:2503.10568*, 2025a.
- 638 Tianhong Li, Yonglong Tian, He Li, Mingyang Deng, and Kaiming He. Autoregressive image
639 generation without vector quantization. *arXiv preprint arXiv:2406.11838*, 2024b.
640
- 641 Yafu Li, Ronghao Zhang, Zhilin Wang, Huajian Zhang, Leyang Cui, Yongjing Yin, Tong Xiao, and
642 Yue Zhang. Lost in literalism: How supervised training shapes translationese in llms, 2025b.
- 643 Yunshui Li, Yiyuan Ma, Shen Yan, Chaoyi Zhang, Jing Liu, Jianqiao Lu, Ziwon Xu, Mengzhao
644 Chen, Minrui Wang, Shiyi Zhan, et al. Model merging in pre-training of large language models.
645 *arXiv preprint arXiv:2505.12082*, 2025c.
646
- 647 Yaron Lipman, Ricky TQ Chen, Heli Ben-Hamu, Maximilian Nickel, and Matt Le. Flow matching
for generative modeling. *arXiv preprint arXiv:2210.02747*, 2022.

- 648 Bingshuai Liu, Longyue Wang, Chenyang Lyu, Yong Zhang, Jinsong Su, Shuming Shi, and
649 Zhaopeng Tu. On the cultural gap in text-to-image generation, 2023.
- 650
651 Haotian Liu, Chunyuan Li, Qingyang Wu, and Yong Jae Lee. Visual instruction tuning. *Advances*
652 *on Neural Information Processing Systems*, 2024a.
- 653 Haozhe Liu, Shikun Liu, Zijian Zhou, Mengmeng Xu, Yanping Xie, Xiao Han, Juan C. Pérez, Ding
654 Liu, Kumara Kahatapitiya, Menglin Jia, Jui-Chieh Wu, Sen He, Tao Xiang, Jürgen Schmidhuber,
655 and Juan-Manuel Pérez-Rúa. Mardini: Masked autoregressive diffusion for video generation at
656 scale. *arXiv preprint arXiv:2410.20280*, 2024b.
- 657
658 Jiasen Lu, Christopher Clark, Sangho Lee, Zichen Zhang, Savya Khosla, Ryan Marten, Derek
659 Hoiem, and Aniruddha Kembhavi. Unified-io 2: Scaling autoregressive multimodal models with
660 vision, language, audio, and action. *arXiv preprint arXiv:2312.17172*, 2023.
- 661 Chuofan Ma, Yi Jiang, Junfeng Wu, Jihan Yang, Xin Yu, Zehuan Yuan, Bingyue Peng, and Xiao-
662 juan Qi. Unitok: A unified tokenizer for visual generation and understanding. *arXiv preprint*
663 *arXiv:2502.20321*, 2025.
- 664
665 Maxime Oquab, Timothée Darcet, Théo Moutakanni, Huy Vo, Marc Szafraniec, Vasil Khalidov,
666 Pierre Fernandez, Daniel Haziza, Francisco Massa, Alaaeldin El-Nouby, et al. Dinov2: Learning
667 robust visual features without supervision. *arXiv preprint arXiv:2304.07193*, 2023.
- 668 Xichen Pan, Satya Narayan Shukla, Aashu Singh, Zhuokai Zhao, Shlok Kumar Mishra, Jialiang
669 Wang, Zhiyang Xu, Jiu Hai Chen, Kunpeng Li, Felix Juefei-Xu, Ji Hou, and Saining Xie. Transfer
670 between modalities with metaqueries. *arXiv preprint arXiv:2504.06256*, 2025.
- 671
672 Ziqi Pang, Tianyuan Zhang, Fujun Luan, Yunze Man, Hao Tan, Kai Zhang, William T. Freeman,
673 and Yu-Xiong Wang. Randar: Decoder-only autoregressive visual generation in random orders.
674 *arXiv preprint arXiv:2412.01827*, 2024.
- 675
676 William Peebles and Saining Xie. Scalable diffusion models with transformers. In *IEEE Interna-*
tional Conference on Computer Vision, 2023.
- 677
678 Aidan Peppin, Julia Kreutzer, Alice Schoenauer Sebag, Kelly Marchisio, Beyza Ermis, John
679 Dang, Samuel Cahyawijaya, Shivalika Singh, Seraphina Goldfarb-Tarrant, Viraat Aryabumi,
680 Aakanksha, Wei-Yin Ko, Ahmet Üstün, Matthias Gallé, Marzieh Fadaee, and Sara Hooker. The
681 multilingual divide and its impact on global ai safety, 2025.
- 682
683 Qi Qin, Le Zhuo, Yi Xin, Ruoyi Du, Zhen Li, Bin Fu, Yiting Lu, Jiakang Yuan, Xinyue Li, Dongyang
684 Liu, et al. Lumina-image 2.0: A unified and efficient image generative framework. *arXiv preprint*
arXiv:2503.21758, 2025.
- 685
686 Aditya Ramesh, Prafulla Dhariwal, Alex Nichol, Casey Chu, and Mark Chen. Hierarchical text-
687 conditional image generation with clip latents. *arXiv preprint arXiv:2204.06125*, 2022.
- 688
689 Aniket Rege, Zinnia Nie, Mahesh Ramesh, Unmesh Raskar, Zhuoran Yu, Aditya Kusupati, Yong Jae
690 Lee, and Ramya Korlakai Vinayak. Cure: Cultural gaps in the long tail of text-to-image systems,
2025.
- 691
692 Robin Rombach, Andreas Blattmann, Dominik Lorenz, Patrick Esser, and Björn Ommer. High-
693 resolution image synthesis with latent diffusion models. In *Conference on Computer Vision and*
Pattern Recognition, 2022.
- 694
695 Israfel Salazar, Manuel Fernández Burda, Shayekh Bin Islam, Arshia Soltani Moakhar, Shivalika
696 Singh, Fabian Farestam, Angelika Romanou, Danylo Boiko, Dipika Khullar, Mike Zhang, et al.
697 Kaleidoscope: In-language exams for massively multilingual vision evaluation. *arXiv preprint*
698 *arXiv:2504.07072*, 2025.
- 699
700 Christoph Schuhmann, Romain Beaumont, Richard Vencu, Cade Gordon, Ross Wightman, Mehdi
701 Cherti, Theo Coombes, Aarush Katta, Clayton Mullis, Mitchell Wortsman, et al. Laion-5b: An
open large-scale dataset for training next generation image-text models. *Advances on Neural*
Information Processing Systems, 2022.

- 702 Team Seawead, Ceyuan Yang, Zhijie Lin, Yang Zhao, Shanchuan Lin, Zhibei Ma, Haoyuan Guo,
703 Hao Chen, Lu Qi, Sen Wang, et al. Seaweed-7b: Cost-effective training of video generation
704 foundation model. *arXiv preprint arXiv:2504.08685*, 2025.
- 705
706 Shivalika Singh, Angelika Romanou, Clémentine Fourier, David I Adelani, Jian Gang Ngui, Daniel
707 Vila-Suero, Peerat Limkonchotiwat, Kelly Marchisio, Wei Qi Leong, Yosephine Susanto, et al.
708 Global mmlu: Understanding and addressing cultural and linguistic biases in multilingual evalu-
709 ation. *arXiv preprint arXiv:2412.03304*, 2024.
- 710 Wei Song, Yuran Wang, Zijia Song, Yadong Li, Haoze Sun, Weipeng Chen, Zenan Zhou, Jian-
711 hua Xu, Jiaqi Wang, and Kaicheng Yu. Dualtoken: Towards unifying visual understanding and
712 generation with dual visual vocabularies. *arXiv preprint arXiv:2503.14324*, 2025.
- 713
714 Keqiang Sun, Juntong Pan, Yuying Ge, Hao Li, Haodong Duan, Xiaoshi Wu, Renrui Zhang, Aojun
715 Zhou, Zipeng Qin, Yi Wang, et al. Journeydb: A benchmark for generative image understanding.
716 *Advances on Neural Information Processing Systems*, 2023a.
- 717 Peize Sun, Yi Jiang, Shoufa Chen, Shilong Zhang, Bingyue Peng, Ping Luo, and Zehuan Yuan.
718 Autoregressive model beats diffusion: Llama for scalable image generation. *arXiv preprint*
719 *arXiv:2406.06525*, 2024.
- 720
721 Quan Sun, Yuxin Fang, Ledell Wu, Xinlong Wang, and Yue Cao. Eva-clip: Improved training
722 techniques for clip at scale. *arXiv preprint arXiv:2303.15389*, 2023b.
- 723
724 Zineng Tang, Ziyi Yang, Chenguang Zhu, Michael Zeng, and Mohit Bansal. Any-to-any generation
725 via composable diffusion. *Advances on Neural Information Processing Systems*, 2023.
- 726
727 Shengbang Tong, David Fan, Jiachen Zhu, Yunyang Xiong, Xinlei Chen, Koustuv Sinha, Michael
728 Rabbat, Yann LeCun, Saining Xie, and Zhuang Liu. Metamorph: Multimodal understanding and
729 generation via instruction tuning. *arXiv preprint arXiv:2412.14164*, 2024.
- 730
731 Hugo Touvron, Thibaut Lavril, Gautier Izacard, Xavier Martinet, Marie-Anne Lachaux, Timothée
732 Lacroix, Baptiste Rozière, Naman Goyal, Eric Hambro, Faisal Azhar, Aurélien Rodriguez, Ar-
733 mand Joulin, Edouard Grave, and Guillaume Lample. Llama: Open and efficient foundation
734 language models. *Computing Research Repository*, 2023.
- 735
736 Eva Vanmassenhove, Dimitar Shterionov, and Andy Way. Lost in translation: Loss and decay of
737 linguistic richness in machine translation. In *Proceedings of Machine Translation Summit XVII:
738 Research Track*, pp. 222–232, Dublin, Ireland, 2019.
- 739
740 Xinlong Wang, Xiaosong Zhang, Zhengxiong Luo, Quan Sun, Yufeng Cui, Jinsheng Wang, Fan
741 Zhang, Yueze Wang, Zhen Li, Qiyang Yu, et al. Emu3: Next-token prediction is all you need.
742 *arXiv preprint arXiv:2409.18869*, 2024.
- 743
744 Shira Wein and Nathan Schneider. Lost in translationese? reducing translation effect using abstract
745 meaning representation. *arXiv preprint arXiv:2304.11501*, 2023.
- 746
747 Chengyue Wu, Xiaokang Chen, Zhiyu Wu, Yiyang Ma, Xingchao Liu, Zizheng Pan, Wen Liu,
748 Zhenda Xie, Xingkai Yu, Chong Ruan, et al. Janus: Decoupling visual encoding for unified multi-
749 modal understanding and generation. In *Conference on Computer Vision and Pattern Recognition*,
750 2025.
- 751
752 Jay Zhangjie Wu, Yixiao Ge, Xintao Wang, Stan Weixian Lei, Yuchao Gu, Yufei Shi, Wynne Hsu,
753 Ying Shan, Xiaohu Qie, and Mike Zheng Shou. Tune-a-video: One-shot tuning of image diffu-
754 sion models for text-to-video generation. In *IEEE International Conference on Computer Vision*,
755 2023a.
- 756
757 Shengqiong Wu, Hao Fei, Leigang Qu, Wei Ji, and Tat-Seng Chua. Next-gpt: Any-to-any multi-
758 modal llm. *arXiv preprint arXiv:2309.05519*, 2023b.
- 759
760 Yecheng Wu, Zhuoyang Zhang, Junyu Chen, Haotian Tang, Dacheng Li, Yunhao Fang, Ligeng
761 Zhu, Enze Xie, Hongxu Yin, Li Yi, et al. Vila-u: a unified foundation model integrating visual
762 understanding and generation. *arXiv preprint arXiv:2409.04429*, 2024.

- 756 Enze Xie, Junsong Chen, Yuyang Zhao, Jincheng Yu, Ligeng Zhu, Chengyue Wu, Yujun Lin, Zhekai
757 Zhang, Muyang Li, Junyu Chen, et al. Sana 1.5: Efficient scaling of training-time and inference-
758 time compute in linear diffusion transformer. *arXiv preprint arXiv:2501.18427*, 2025a.
- 759
760 Jinheng Xie, Yuexiang Li, Yawen Huang, Haozhe Liu, Wentian Zhang, Yefeng Zheng, and
761 Mike Zheng Shou. Boxdiff: Text-to-image synthesis with training-free box-constrained diffu-
762 sion. In *IEEE International Conference on Computer Vision*, 2023.
- 763
764 Jinheng Xie, Weijia Mao, Zechen Bai, David Junhao Zhang, Weihao Wang, Kevin Qinghong Lin,
765 Yuchao Gu, Zhijie Chen, Zhenheng Yang, and Mike Zheng Shou. Show-o: One single trans-
766 former to unify multimodal understanding and generation. *International Conference on Learning
Representations*, 2025b.
- 767
768 An Yang, Baosong Yang, Beichen Zhang, Binyuan Hui, Bo Zheng, Bowen Yu, Chengyuan Li,
769 Dayiheng Liu, Fei Huang, Haoran Wei, Huan Lin, Jian Yang, Jianhong Tu, Jianwei Zhang,
770 Jianxin Yang, Jiayi Yang, Jingren Zhou, Junyang Lin, Kai Dang, Keming Lu, Keqin Bao, Kexin
771 Yang, Le Yu, Mei Li, Mingfeng Xue, Pei Zhang, Qin Zhu, Rui Men, Runji Lin, Tianhao Li,
772 Tingyu Xia, Xingzhang Ren, Xuancheng Ren, Yang Fan, Yang Su, Yichang Zhang, Yu Wan,
773 Yuqiong Liu, Zeyu Cui, Zhenru Zhang, and Zihan Qiu. Qwen2.5 technical report. *arXiv preprint
arXiv:2412.15115*, 2024.
- 774
775 Lijun Yu, José Lezama, Nitesh B Gundavarapu, Luca Versari, Kihyuk Sohn, David Minnen, Yong
776 Cheng, Vighnesh Birodkar, Agrim Gupta, Xiuye Gu, et al. Language model beats diffusion-
777 tokenizer is key to visual generation. *arXiv preprint arXiv:2310.05737*, 2023.
- 778
779 Xiang Yue, Yueqi Song, Akari Asai, Seungone Kim, Jean de Dieu Nyandwi, Simran Khanuja, Anjali
780 Kantharuban, Lintang Sutawika, Sathyanarayanan Ramamoorthy, and Graham Neubig. Pangea:
781 A fully open multilingual multimodal llm for 39 languages. In *International Conference on Learn-
ing Representations*, 2024.
- 782
783 David Junhao Zhang, Jay Zhangjie Wu, Jia-Wei Liu, Rui Zhao, Lingmin Ran, Yuchao Gu, Difei
784 Gao, and Mike Zheng Shou. Show-1: Marrying pixel and latent diffusion models for text-to-
785 video generation. *arXiv preprint arXiv:2309.15818*, 2023.
- 786
787 Chunting Zhou, LILI YU, Arun Babu, Kushal Tirumala, Michihiro Yasunaga, Leonid Shamis, Jacob
788 Kahn, Xuezhe Ma, Luke Zettlemoyer, and Omer Levy. Transfusion: Predict the next token and
789 diffuse images with one multi-modal model. In *International Conference on Learning Represen-
tations*, 2025.
- 790
791
792
793
794
795
796
797
798
799
800
801
802
803
804
805
806
807
808
809

A APPENDIX

A.1 MORE ON RELATED WORKS

Large multimodal models. Recent advances in large multimodal models (LMMs) (Liu et al., 2024a; Chen et al., 2024b; Li et al., 2024a; Bai et al., 2025; Dash et al., 2025) have extended large language models (LLMs) (Touvron et al., 2023; Yang et al., 2024) to support image understanding tasks, including image captioning and visual question answering. These models typically rely on a vision encoder to extract image features, which are then projected into the LLM embedding space for cross-modal alignment. More recent encoder-free models (Xie et al., 2025b; Diao et al., 2024; 2025) bypass the explicit image encoder and instead align raw visual tokens directly within the LLM space. Among early efforts to enable multilingual visual understanding, Maya (Alam et al., 2024; 2025), Aya-Vision (Dash et al., 2025) and Pangea (Yue et al., 2024) incorporate a multilingual training corpus. However, they are limited to image understanding tasks. In contrast, our proposed NEOBABEL architecture focuses exclusively on multilingual image generation, offering the first encoder-free model that aligns visual features in the LLM space while supporting cross-lingual generation. Architecturally, NEOBABEL is closely related to show-o (Xie et al., 2025b), sharing the same design goal of direct visual alignment in language space, but differs in its task focus and multilingual design.

A.2 TRAINING DETAILS

Each stage is trained for 500k steps (except the final stage of instruction tuning with 200k) using the AdamW optimizer and cosine learning rate decay. The learning rate is set to $1e-4$ during pretraining and adjusted during instruction tuning. We gradually increase prompt sequence length and resolution from 128 to 512 and from 256×256 to 512×512 respectively. The vocabulary and codebook sizes are fixed across all stages. To further stabilize training and improve generalization, we merge checkpoints across the trajectory, with Simple Moving Average emerging as the most effective strategy (see Sections A.3 and A.4).

Table 4: Hyperparameters across training progression.

Hyperparameters	Pretraining			Instruction Tuning	
	1st Stage	2nd Stage	3rd Stage	1st Stage	2nd Stage
Training Steps	500k	500k	500k	500k	200k
Warmup Steps	5000	5000	5000	5000	2000
Learning Rate	$1e-4$	$1e-4$	$1e-4$	$2e-4$	$5e-5$
Learning Rate Decay	cosine	cosine	cosine	cosine	cosine
Optimizer	AdamW	AdamW	AdamW	AdamW	AdamW
Image Resolution	256×256	256×256	256×256	512×512	512×512
LLM Sequence Length	128	512	512	512	512
LLM Vocab Size	256k	256k	256k	256k	256k
Codebook Size	8192	8192	8192	8192	8192

A.3 MULTILINGUAL MODEL MERGING

To enhance generalization and stability of multilingual image generation models, we adopt model merging techniques that combine multiple checkpoints from the training trajectory. Let $\{M_i\}_{i=1}^N$ denote a sequence of N model checkpoints and $\{w_i\}_{i=1}^N$ their corresponding non-negative weights. The merged model \widehat{M} is defined as a convex combination:

$$\widehat{M} = \sum_{i=1}^N \alpha_i M_i \quad \text{where} \quad \alpha_i = \frac{w_i}{\sum_{j=1}^N w_j}. \quad (1)$$

This formulation allows the merged model to interpolate within the solution space spanned by the selected checkpoints, potentially improving generalization on unseen prompts and enhancing robustness to overfitting. We consider three widely used weighting strategies for this purpose, each

reflecting different assumptions about model evolution during training. The comparative results and analysis of these approaches are presented ablation studies section.

Simple Moving Average (SMA) assigns equal weight to all checkpoints. It is defined as:

$$M_{\text{avg}} = \frac{1}{N} \sum_{i=1}^N M_i. \quad (2)$$

SMA is simple, stable, and particularly effective when applied in the later stages of training where model weights exhibit minimal drift. Prior work (Li et al., 2025c) found SMA to perform robustly due to this stabilization.

Exponential Moving Average (EMA) emphasizes recent checkpoints by applying exponentially decaying weights. It is computed recursively as:

$$M_{\text{avg}}^{(i)} = \alpha M_i + (1 - \alpha) M_{\text{avg}}^{(i-1)}, \quad i \in [2, N]. \quad (3)$$

The decay factor $\alpha \in (0, 1)$ controls the trade-off between recency and stability. EMA adapts more quickly to recent model dynamics but is sensitive to noise if weights are unstable.

Weighted Moving Average (WMA) assigns custom, possibly increasing weights to later checkpoints. The merged model is computed using the normalized form:

$$M_{\text{avg}} = \sum_{i=1}^N \frac{w_i}{w_{\text{sum}}} M_i, \quad \text{where } w_{\text{sum}} = \sum_{i=1}^N w_i. \quad (4)$$

This general formulation allows flexibility in how much importance is placed on each checkpoint. In our case, we use $w_i = i$ to emphasize later-stage models.

A.4 EFFECT OF MODEL MERGING ON GENERALIZATION

We investigate the impact of model merging on multilingual image generation performance by combining $N = 20$ checkpoints sampled at 10,000-step intervals from the second instruction tuning stage (steps 0–200K). Table 5 reports the results of three merging strategies: Simple Moving Average (SMA), Exponential Moving Average (EMA), and Weighted Moving Average (WMA) compared to the last checkpoint baseline. As reported, m-GenEval score on English prompt improves from 0.81 to 0.83 after model merging. Both WMA and SMA reach this upper bound, indicating that merging checkpoints along the optimization path enhances semantic alignment. Moreover, m-DPG score on English prompt remains stable or show modest gains, suggesting that merging preserves the model’s ability to accurately follow dense, attribute-rich prompts without sacrificing fine-grained multilingual grounding. Among the merging strategies, SMA performs best overall due to its uniform averaging over well-aligned checkpoints. EMA also improves results but remains more susceptible to short-term training noise. WMA offers a compromise by emphasizing later checkpoints, trading off stability for adaptability. These findings underscore that checkpoint merging can meaningfully enhance both compositional understanding and multilingual robustness, with SMA offering a simple yet effective strategy.

Table 5: Effect of model merging on generalization. All merging strategies improve performance on m-GenEval and slightly enhance m-DPG, highlighting model merging as a simple yet effective way to boost generalization.

Method	m-GenEval	m-DPG
Last checkpoint	0.81	0.73
EMA	0.82	0.75
WMA	0.83	0.75
SMA	0.83	0.75

A.5 DATA FILTERING

In this section, we describe in detail the four post-processing and filtering strategies: length filtering, language validation, visual–text mismatch filtering, and toxicity/NSFW filtering, used to ensure dataset quality and consistency across languages.

- **Length filtering:** Remove captions that are too short (e.g., fewer than 5 tokens) or excessively long (e.g., more than 500 tokens).

- **Language validation:** Detect and discard captions containing non-English phrases or corrupted outputs using language identification tools. We use the `fastText` language identification model trained on 176 languages (Joulin et al., 2016). We discard any caption not classified as English with a confidence score above 90%.
- **Visual-text mismatch filtering:** Discard captions that do not align with visual content, measured via auxiliary vision-language models (e.g., using VQAScore). Specifically, we leverage MolMo-72B (Deitke et al., 2025) deployed with vLLM (Kwon et al., 2023), formulating the task as a binary structured prediction (`yes/no`) via vLLM’s output interface.
- **Toxicity and NSFW filtering:** Discard samples using the LAION-5B NSFW classifier (Schuhmann et al., 2022) to ensure safe visual content before captioning, assuming high likelihood of appropriateness in the resulting captions.

A.6 CODE-SWITCHING SIMILARITY (CSS)

Definition. A multilingual model should demonstrate robustness not only to monolingual prompts but also to mixed-language inputs i.e. to code-switching. Code switching often increases perplexity and degrades performance in language models; however, its impact on image generation remains largely unexplored. To evaluate this, we introduce the CSS Score, which quantifies visual consistency under intra-prompt language variation. Given a set of reference prompts in English, we construct two variants per prompt for each of the $L-1$ non-English target languages: (1) `English-First (EF)`: the first half of the prompt remains in English while the second half is translated into the target language, and (2) `English-Second (ES)`: the first half is translated while the second half remains in English. For each prompt $p \in \{p_i\}_{i=1}^P$, we generate a single reference image x_{ref} from the original English prompt and $L-1$ code-switched images: $x_{\text{EF}}^{(l)}$ and $x_{\text{ES}}^{(l)}$ for each target language l . Each image is encoded into an embedding $f(x) \in \mathbb{R}^d$ using a vision encoder. The Code Switching Similarity (CSS) score for each prompt is computed by measuring the average cosine similarity between the reference embedding $f(x_{\text{ref}})$ and the embeddings from the EF and ES variants:

$$\text{CSS}_{p^{\text{EF}}} = \frac{1}{L-1} \sum_{l=1}^{L-1} \cos \left(f(x_{\text{ref}}), f(x_{\text{EF}}^{(l)}) \right), \quad \text{CSS}_{p^{\text{ES}}} = \frac{1}{L-1} \sum_{l=1}^{L-1} \cos \left(f(x_{\text{ref}}), f(x_{\text{ES}}^{(l)}) \right). \quad (5)$$

The final CSS scores are obtained by averaging across all prompts. To assess how well models preserve semantic consistency under intra-prompt code switching, we report both CSS^{EF} and CSS^{ES} , using embeddings from EVA-CLIP (Sun et al., 2023b) and DINOv2 (Oquab et al., 2023) computed on m-DPG prompts.

Analysis. We assess the CSS score with EVA-CLIP and DINOv2. As shown in Table 6, NEOBABEL outperforms larger models under both English-First (EF) and English-Second (ES) prompts. EVA-CLIP scores show minimal EF-ES differences, indicating limited impact of English segment position on semantic alignment, while DINOv2 scores are consistently lower, reflecting the greater challenge of maintaining structural coherence under language mixing. A robust model should achieve both high CSS and small EF-ES gaps, a balance met by NEOBABEL with 0.82/0.81 on EVA-CLIP and 0.67/0.64 on DINOv2. Figure 9 further shows that, unlike BLIP3-o (8B) which exhibits high variance across prompts, NEOBABEL combines higher medians with lower dispersion, confirming its consistent handling of code-mixed inputs. These results demonstrate that effective multilingual alignment, not parameter count, is key to robustness under code switching.

A.7 USE OF LARGE LANGUAGE MODELS

We used large language models exclusively for grammar correction and language refinement of the manuscript. It played no role in research ideation, methodological design, experimentation, data analysis, or result generation; all technical content was solely developed and validated by the authors.

Table 6: **Code Switching Similarity (CSS) analysis** using EVA-CLIP and DINOv2 backbones. Scores are reported for two prompt variants: English First (EF) and English Second (ES). NEO-BABEL (2B) outperforms larger models, showing strong visual consistency and robustness to code-mixed input order. The larger DINOv2 gap reflects its higher sensitivity to visual-structural variation, while EVA-CLIP remains more stable due to its semantic focus.

Model	Params	EVA-CLIP		DINOv2	
		EF	ES	EF	ES
Show-o	1.3B	0.73	0.72	0.41	0.38
Janus	1.3B	0.75	0.73	0.50	0.43
Janus Pro	7B	0.76	0.72	0.58	0.50
BLIP3-o	4B	0.75	0.75	0.54	0.54
BLIP3-o	8B	0.74	0.74	0.52	0.51
NEOBABEL	2B	0.82	0.81	0.67	0.64

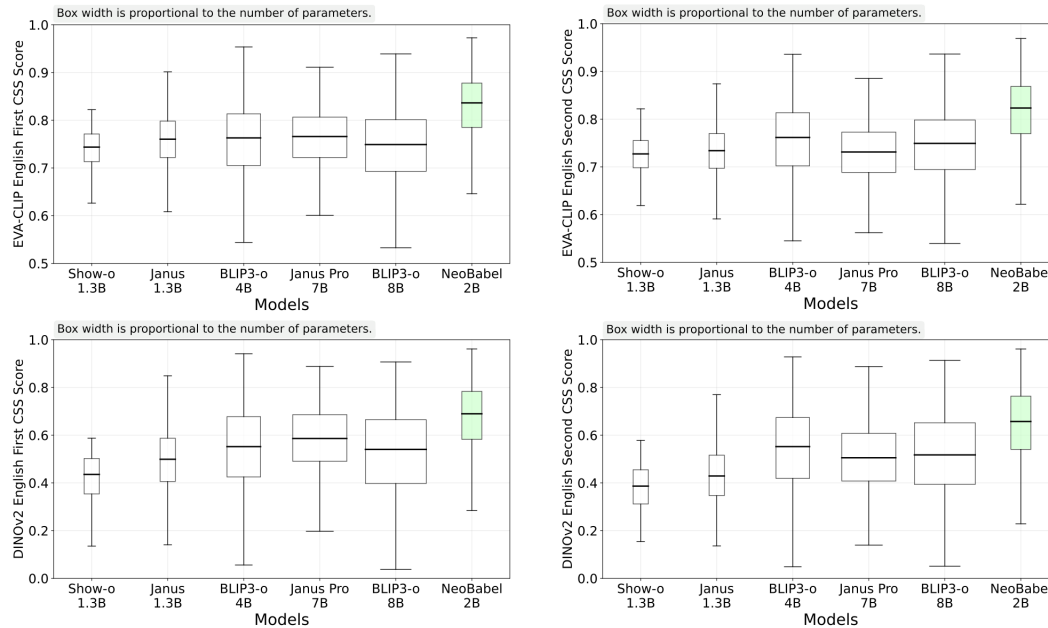


Figure 9: **Variation in Code Switching Similarity (CSS) scores across models.** We report CSS scores for code-mixed prompts under two settings: English-first (left column) and English-second (right column), using EVA-CLIP (top row) and DINOv2 (bottom row) as backbones. Higher scores indicate stronger visual alignment with the reference image, while smaller EF-ES gaps suggest robustness to code-switch position. NEOBABEL consistently achieves higher medians and lower variance than larger baselines, especially under DINOv2, highlighting its effective and stable handling of multilingual prompts.

1026
1027
1028
1029
1030
1031
1032
1033
1034
1035
1036
1037
1038
1039
1040
1041
1042
1043
1044
1045
1046
1047
1048
1049
1050
1051
1052
1053
1054
1055
1056
1057
1058
1059
1060
1061
1062
1063
1064
1065
1066
1067
1068
1069
1070
1071
1072
1073
1074
1075
1076
1077
1078
1079

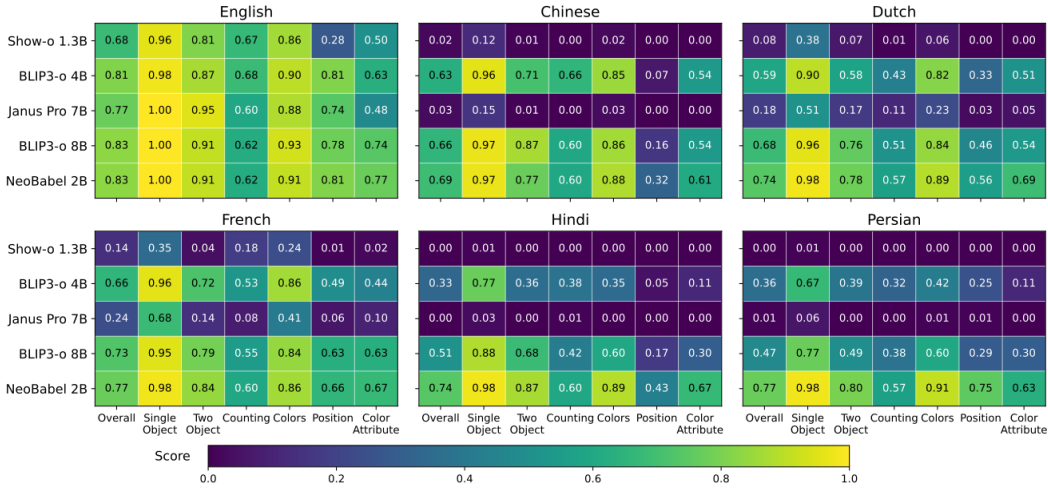


Figure 10: **m-GenEval benchmark comparison.** Models such as Janus Pro and BLIP3-o rely on multilingual base LLMs but are trained solely on English image-generation data, leading to a sharp performance drop in non-English languages. In contrast, NEOBABEL maintains strong and consistent results across all languages, demonstrating robust cross-lingual generalization.

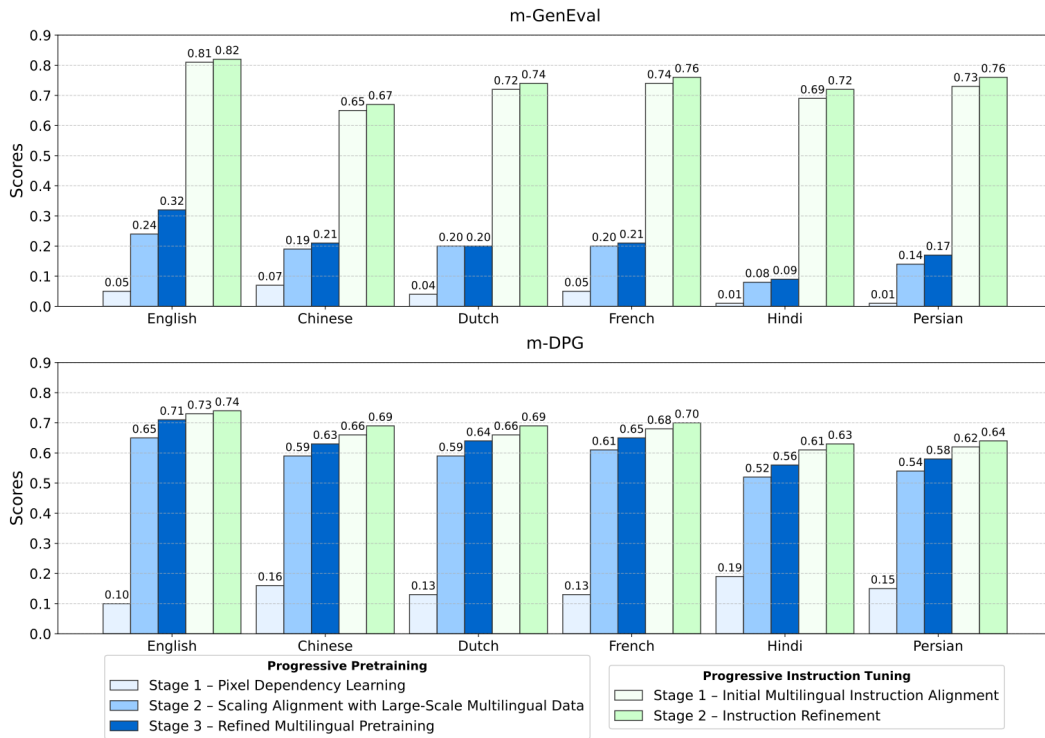


Figure 11: **Effect of progressive pretraining and instruction tuning.** Performance on m-GenEval (top) and m-DPG (bottom) improves steadily across pretraining and instruction tuning stages.

1080
1081
1082
1083
1084
1085
1086
1087
1088
1089
1090
1091
1092
1093
1094
1095
1096
1097
1098
1099
1100
1101
1102
1103
1104
1105
1106
1107
1108
1109
1110
1111
1112
1113
1114
1115
1116
1117
1118
1119
1120
1121
1122
1123
1124
1125
1126
1127
1128
1129
1130
1131
1132
1133

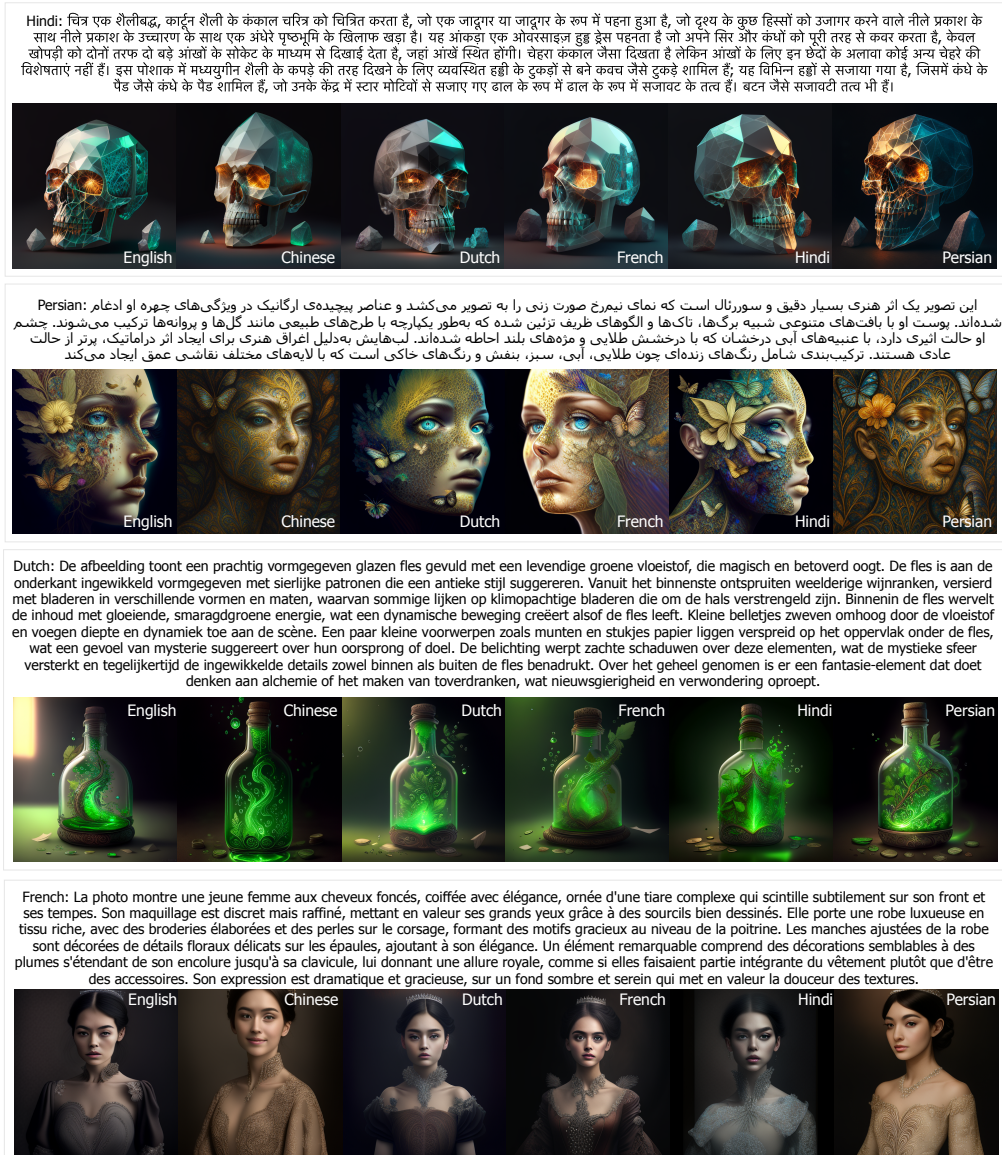
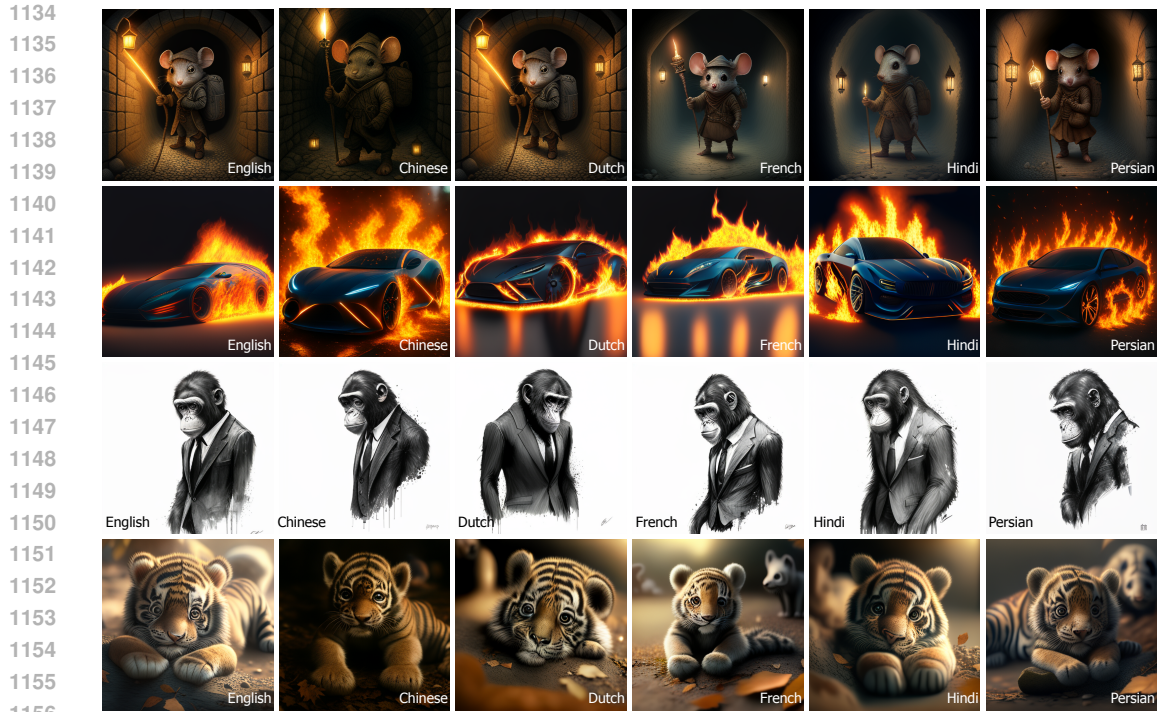


Figure 12: **Qualitative evaluation of NEOBABEL.** Each row is based on a single concept expressed in six different languages. We show only one of the prompts (in one language) and present six images generated from its translated prompts in the other five languages. Across all languages, NEOBABEL delivers semantically accurate and visually cohesive outputs with reliable consistency.



1157 **Figure 13: Qualitative evaluation of NEOBABEL.** Each row corresponds to a single concept expressed in six different languages: English, Chinese, Dutch, French, Hindi, and Persian. Although prompts are not shown for readability, all images were generated using translated versions of the same underlying prompt in each language. NEOBABEL consistently produces semantically aligned and visually coherent results across languages, highlighting its strong multilingual generation capabilities. We intentionally omit the prompts here due to their length, focusing instead on the visual consistency across languages.

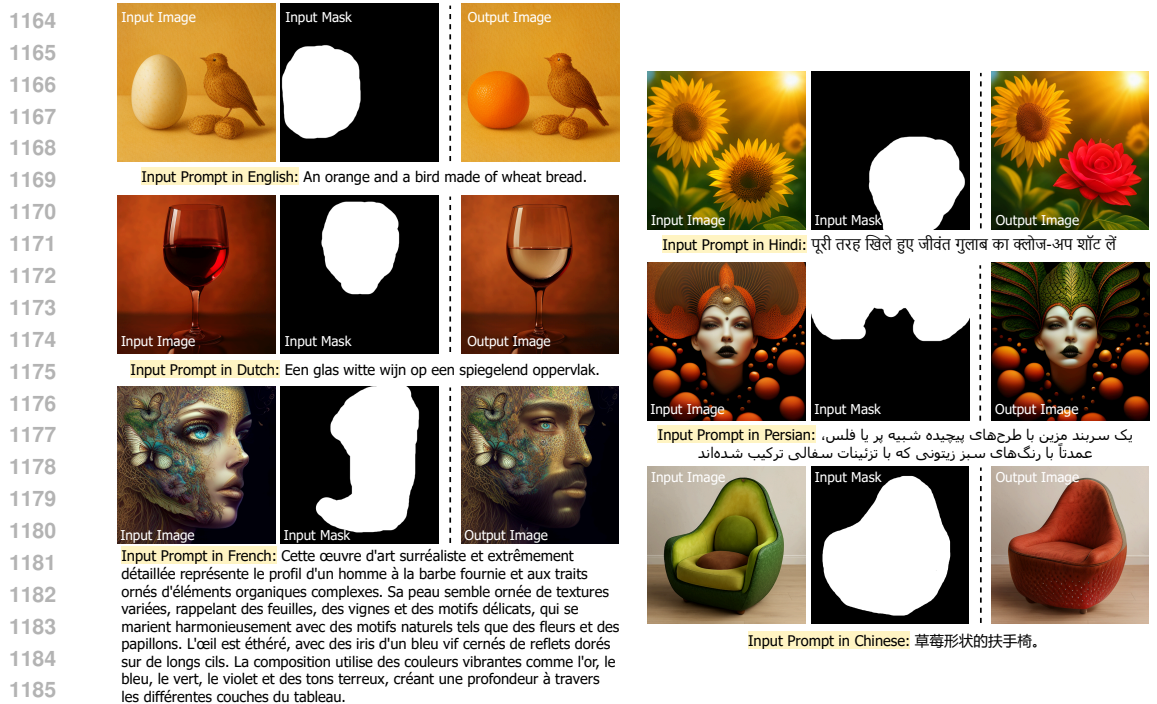


Figure 14: Multilingual image inpainting. NEOBABEL supports multilingual text-guided image inpainting, highlighting its potential for interactive visual editing across diverse user groups.

1188
1189
1190
1191
1192
1193
1194
1195
1196
1197
1198
1199
1200
1201
1202
1203
1204
1205
1206
1207
1208
1209
1210
1211
1212
1213
1214
1215
1216
1217
1218
1219
1220
1221
1222
1223
1224
1225
1226
1227
1228
1229
1230
1231
1232
1233
1234
1235
1236
1237
1238
1239
1240
1241

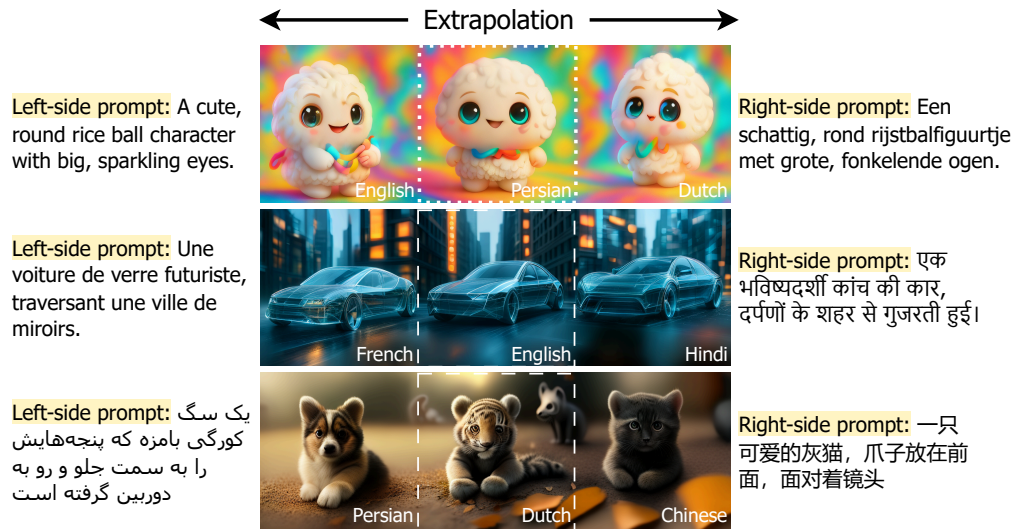


Figure 15: **Multilingual image extrapolation.** NEOBABEL performs text-guided image extrapolation, generating coherent left and right extensions from different multilingual prompts.

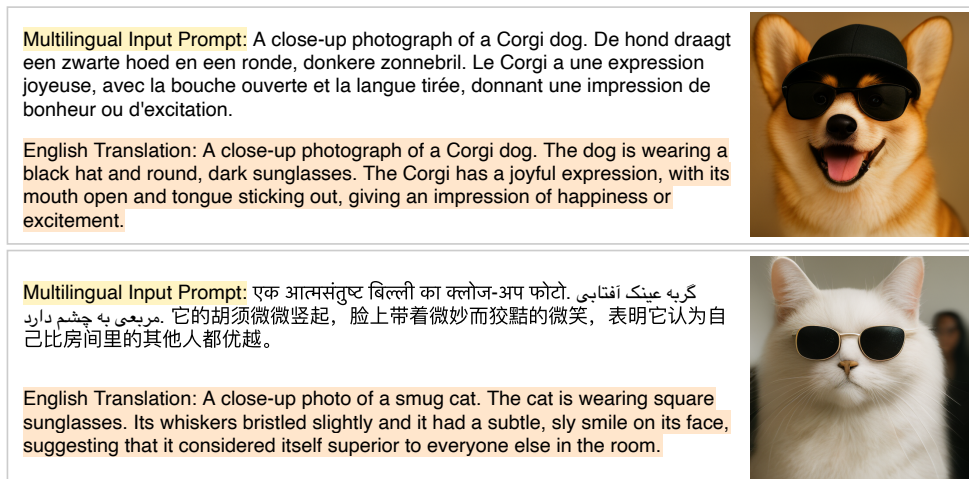


Figure 16: **Cross-Lingual Prompt Generation.** An example of a code-switched prompt combining English, Dutch, and French, with the image generated by NEOBABEL. English translations are shown for reader convenience, they are not used as input.